Fibers and Polymers 2018, Vol.19, No.6, 1335-1346
DOI 10.1007/s12221-018-1009-4

ISSN 1229-9197 (print version)
ISSN 1875-0052 (electronic version)

Effect of Compatibilizer on the Properties of Polyamide 6 Blend Based Carbon Fiber Reinforced Composites

S. Aparna, D. Purnima*, and R.B. Adusumalli

Department of Chemical Engineering, Birla Institute of Technology and Science-Pilani, Hyderabad Campus, Hyderabad, Telangana 500078, India

(Received November 23, 2017; Revised April 6, 2018; Accepted April 30, 2018)

Abstract: Carbon fiber composites are preferred in transportation sector due to their high specific strength, modulus and resistance to corrosive environments. This paper reports on usage of Polyamide 6 in automobile exterior components by adding 30 % PP, *PP-g-MA* (Polypropylene-grafted-Maleic anhydride) as a compatibilizer and Short Carbon fibers (SCF) as reinforcement. The effect of compatibilizer on the tensile and impact properties of the composites has been studied. Composite with 3 phr *PP-g-MA* and 5 wt% SCF revealed highest tensile strength and only 10 % reduction in its value due to water saturation. Microstructure analysis and Grey relational analysis confirmed the experimental results.

Keywords: Polyamide 6/PP blend, *PP-g-MA* compatibilizer, Carbon fibers, Injection molded composites, Tensile test, Grey relational analysis

Introduction

Polyamide 6 (PA6 or Nylon 6) is a tough engineering plastic known for its low density, low dielectric constant, high tensile strength and high thermal stability [1,2]. It is used mainly in automobile and aerospace application [1-3] and also as ropes, films and boil-in bags because of its good barrier property and high toughness. PA6 has been increasingly studied as a matrix material for making carbon fiber (CF) reinforced composites using various processing methods viz. extrusion, injection molding, compression molding, laminate forming and in-situ anionic polymerization of PA6 with CF [1-8]. The property of the composite depends on nature of PA6 (molecular weight, Melt Flow Index (MFI), terminal groups), nature of CF (short, nonwoven, woven mats), content of CF (2 wt % to 40 wt %) and processing condition (temperature, pressure, speed of the screw). PP (Polypropylene) is known for its low melting point, low density (lower than PA6), and hydrophobicity [9]. PP is added to PA6 with the objective of reducing its water intake during service (high humid applications) and to ease the processability of PA6.

PA6/PP forms immiscible blends due to the hydrophilic and hydrophobic nature of PA6 and PP respectively. For better dispersion of PP and for improvement of interfacial adhesion between PA6 and PP, compatibilizers are used. Hence addition of compatibilizer affects the properties such as, impact strength, tensile strength and toughness of the blends. From the earlier reports [10-17], it has been deduced that MA (Maleic anhydride) is the most suitable functional group for compatibilization of PA6/PP blend as MA reactively compatibilizes with PA6 by reacting with the -NH_2- end group of PA6. *SEBS-g-MA* (Styrene Ethylene Butylene Styrene-grafted-MA), *EPR-g-MA* (Ethylene Propylene Rubber-g-MA) and *PP-g-MA* have been used as compatibilizers for PA6/PP blends [10-13,18-20]. Addition of *SEBS-g-MA* and *EPR-g-MA* led to increase in impact strength but reduction in tensile strength of PA6/PP blend. Hence *PP-g-MA* was studied as compatibilizer to minimize the loss of tensile strength. CF is usually added to the blends as a reinforcement due to its high tensile strength, stiffness, conductivity and high resistance to temperature, moisture and corrosive environments. CF has been studied as reinforcement in various forms including short carbon fibers (SCF) of 0.5, 1, 2, 5, 10 mm lengths, long fibers and bidirectional mats which leads to increase in tensile strength and tensile modulus of PA6 and/or PP composites [21,22]. The percentage increase in tensile strength depends on various factors including residual fiber length, fiber orientation, fiber volume content and sizing agent [1-8,23,24].

PP-g-MA has not been widely studied as compatibilizer for hybrid composite though compatibilizer plays a major role in determining the properties of the blends and composites [25]. Fiber reinforced composites based on PA6 blend i.e. PA6/PPS/SCF without compatibilizer [4], PA6/TPU (Thermoplastic Urethane)/CF [26], PA6/ABS (Acrylonitrile butadiene styrene)/*ABS-g-MA*/SGF (Short glass fiber) [27] were studied in detail. Do *et al*. [23] studied the effect of PP content on PA6/PP/SCF composite with *PP-g-MA* as compatibilizer for PA6 composite that could be used for high humid application. In previous studies [23,25,28,29], 70/30 wt/wt of PA6/PP has been used as matrix material for composites to obtain better interaction between PA6/PP and to have better properties after water saturation. But the effect of *PP-g-MA* on morphology and mechanical properties of PA6/PP/SCF composite was not studied to the best of author's knowledge. Since under water applications like marine pressure vessels, composite conduits [30], automobile exterior components require strength in wet condition and battery & fuel cell require electrical conductivity in dry

*Corresponding author: dpurnima@hyderabad.bits-pilani.ac.in

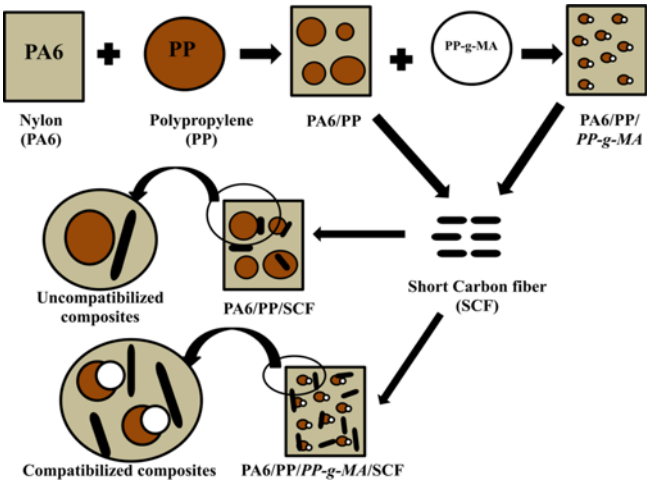

Figure 1. Schematic diagram representing the effect of *PP-g-MA* on PA6/PP blend and composite.

condition, it is important to study isotropic composite of high strength, high toughness and/or high electrical conductivity such as SCF reinforced PA6/PP composites. Here isotropic corresponds to lower SCF content, because carbon fibers are anisotropic.

In this paper, the effect of compatibilizer on PA6/PP blend based composites was studied in detail using 70/30 wt/wt. The compatibilizer (*PP-g-MA*) content is varied between 0-5 phr and properties of PA6/PP/*PP-g-MA*/SCF have been studied in comparison with pure PA6, PA6/PP and PA6/PP/*PP-g-MA*. The Figure 1 schematically illustrates the PA6, blends & composites and effect of *PP-g-MA* on blends and composites. The SCF content is restricted to 5 wt % because carbon fibers have higher tensile properties (~4.5 GPa of strength & ~200 GPa of stiffness) and it is easy to disperse the fibers uniformly in a matrix via extrusion and injection molding. The other reason is that with increase in fiber content, the residual fiber length decreases i.e. losing the effect of reinforcement [22]. In this study SCF of 1 mm length, diameter of 7 μm, 5 wt % is used. PA6, its blends and composite were prepared by first mixing in a twin-screw extruder and then injection molding in order to make homogeneous and isotropic composites (due to lower amount of SCF) which could maintain its strength even at higher humidity condition. Effect of compatibilizer content on tensile properties of composites was studied before water absorption (BWA) and after water absorption (AWA) or water saturation. Impact studies were restricted to dry (BWA) samples only. Morphology of the tensile fractured specimen was also studied using SEM to correlate it with the tensile properties. Statistical analysis was carried out using Grey relational analysis (GRA) to find the optimum compatibilizer content. Finally residual fiber length of the composite was determined using matrix burn-off method and surface polishing method.

Experimental

Materials

PA6 of grade GUJLON M28RC (Melt flow index: 35 g/10 min at 230 °C, 2.16 kg load) was obtained from Gujarat State Fertilizer & Chemicals Ltd., India and PP of grade H030SG (Melt flow index: 3.4 g/10 min at 230 °C, 2.16 kg load; tensile strength: 34 MPa) was obtained from Reliance Industries Ltd., India. Short carbon fiber (SCF) with 1 % epoxy coating having average length of 1 mm and average diameter of 7 μm, was obtained from Sun Young industry, South Korea and *PP-g-MA* of grade OPTIM-408 with very high MA content (Melt flow index: 50 g/10 min at 190 °C, 2.16 kg load) was obtained from Pluss Polymers Limited, India. Laboratory grade extra pure Xylene, Bromo thymol blue, Potassium Hydroxide and Ethyl alcohol used for titration were procured from SDFCL, India.

Estimation of Maleic Anhydride (MA) Content

MA content in *PP-g-MA* was determined using titration method, as stated by Oromiehie *et al*. [31]. 0.5 g of *PP-g-MA* was dissolved in 50 m*l* of xylene at 80 °C, and 1 m*l* of water was added in order to hydrolyze the maleic anhydride to maleic acid, which was then titrated against alcoholic KOH (0.1 N). Bromo thymol blue was used as indicator. The end point was change of color from yellow to sky blue. The grafting percentage was calculated from the acid number value generated from the titration as given in equation (1) and (2).

$$G = (A.N \times M_m) / (2 \times 561) \quad (1)$$

$$A.N = (mlKOH \times N \times 56.1) / gr.polymer \quad (2)$$

where, G is the MA grafting percentage, $A.N$ is the acid number, M_m is the molecular weight of the monomer to which MA is grafted and *mlKOH* is the alcoholic KOH consumed for neutralizing the maleic acid present in 0.5 gram of *PP-g-MA* and N is the normality of the alcoholic KOH. Grafted MA content was determined to be 1.375 % for *PP-g-MA* used in this study.

Compounding of the Blends and Composite

All materials shown in Figure 2(a)-(d) were preheated for 5 hours at 80 °C in hot air oven, and then extruded in Berstorff Maschinenban (ZE-25 GmbH, Germany) which is a co-rotating twin screw extruder with L/D ratio 48, screw diameter 25 mm and screw speed 100 rpm. Temperature of screw gradually increased from zone-1 to zone-7 as 170 °C, 180 °C, 190 °C, 210 °C, 220 °C, 230 °C, and 235 °C at the die. The profile (Figure 2(e)) coming out of the extruder was cooled in a water bath and pelletized (Figure 2(f)). Same temperature profile and screw speed were maintained for compounding all compositions i.e. PA6, PA6/PP (blends) and composites. For blends, all materials were tumbled and

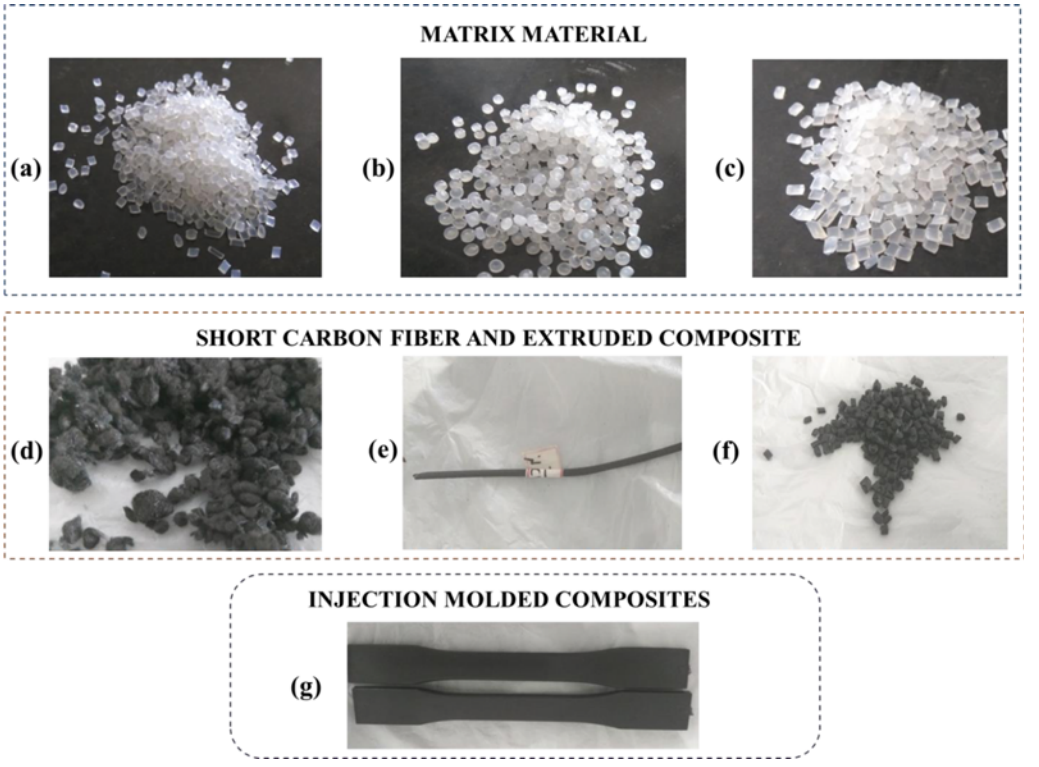

Figure 2. (a) PA6 pellets (d=2 mm), (b) PP pellets (d=4 mm), (c) *PP-g-MA* pellets (d=2.5 mm), (d) Carbon fibers of 1 mm length, (e) Composite rod of 3 mm diameter obtained from extrusion (f) pellets of composite (d=3 mm, l=4 mm) and (g) Injection molded specimens of composite (NPMC5).

Table 1. Composition of blends and composites. SCF-short carbon fiber and MA-maleic anhydride, phr-parts per hundred parts of resin

Sample name	PA6 (wt %)	PP (wt %)	*PP-g-MA* (phr)	SCF (wt %)
N	100	-	-	-
NP	70	30	-	
NPM	70	30	4	-
NPMC0	70	30	-	5
NPMC3	70	30	3	5
NPMC4	70	30	4	5
NPMC5	70	30	5	5

Note: N-PA6, NP-PA6/PP, NPM- PA6/PP/*PP-g-MA*, NPMC0-PA6/PP/SCF, NPMC3 to NPMC5-PA6/PP/*PP-g-MA*/SCF.

added to hopper directly. For composites, the plastic pellets were added to hopper, and SCF was fed through feeder located at middle part of zone-1 at around 170 °C. Details of compositions studied are given in Table 1.

Injection Molding of the Composite Pellets

The pellets obtained from extrusion process were oven dried for 5 hrs at 90 °C and injection molded to make dog bone specimens of 3.2 mm thickness required for tensile testing (Figure 2(g), ASTM D638). Electronica Endura-90 injection molding machine was used to make all specimens with temperature range of 49 °C to 249 °C from the compression zone to the nozzle with cycle time of 40 seconds and injection pressure of 784 bar. Pellets of pure PA6, PA6/PP (blends) and composites were processed to make specimens for tensile test and impact test.

Water Absorption (saturation) Test

Water absorption was carried out for tensile specimen according to ASTM D570-98 standard. The tensile specimens of PA6, PA6 blends and composites were immersed in distilled water at room temperature and weighed every 24 hours until saturation occurred using electronic weighing balance (Sartorius BSA-423S-CW). Samples were removed from water bath and their weight was measured after surface drying using tissue paper. The level of water was maintained at same level to ensure proper saturation. The weight difference was found and the percentage increase in weight which is proportional to the amount of water absorbed was calculated using equation (3).

$$\%W = \frac{W_n - W_0}{W_0} \times 100 \quad (3)$$

where, W_0 is the initial weight of the sample, W_n is the

Table 2. Influence of water absorption on weight and tensile properties

Sample	% Increase in weight	% Reduction in tensile strength	% Increase in elongation	% Reduction in tensile modulus
N	6.2	37.1	11	71.9
NP	2.9	53	519.7	72.7
NPM	2.5	44.7	160	52.6
NPMC0	2.2	22.3	23.7	47.7
NPMC3	2.4	10.7	56.1	30.9
NPMC4	2.4	18.8	53.6	37.7
NPMC5	2.2	20.7	51	30.5

Note: N-PA6, NP-PA6/PP, NPM- PA6/PP/*PP-g-MA*, NPMC0-PA6/PP/SCF, NPMC3 to NPMC5- PA6/PP/*PP-g-MA*/SCF.

weight of the saturated sample, and %*W* gives the percentage increase in weight as shown in Table 2.

Mechanical Properties

The tensile test was carried out using Micro-control systems Universal Testing Machine at a crosshead speed of 5 mm/min and a gauge length of 70 mm as per ASTM D638 standard. Tensile properties of all dog bone specimens were studied before (BWA) and after water absorption (AWA). AWA samples were tested after 45 days of water saturation and tested immediately after surface drying. During the test, few AWA specimens elongated beyond 300 %. Tensile strength, modulus and % elongation were obtained from the stress-strain plots. The notched-izod impact test was conducted as per ASTM D256 standard on (CEAST 9050) pendulum type impact tester for all compositions. Flat specimens of 3.2 mm thickness and 64 mm length obtained from injection molding were used for impact test (BWA). Both tests were carried out at 23-25 ^{o}C and 50-55 % relative humidity to avoid the influence of relative humidity on mechanical properties.

FTIR (Fourier Transformed Infrared) Analysis

For FTIR analysis, thin slices were peeled from both sides of injection molded specimens using blade which was then fragmented into small particles suitable for FTIR analysis using scissor. The small particles or powdered samples were mixed with potassium bromide to form pellets required for the FTIR analysis. The blends and composites were tested and analyzed using Jasco-FTIR4200 equipment.

Analysis Using Scanning Electron Microscopy (SEM), Optical Microscopy (OM) and Confocal Laser Scanning Microscopy (CLSM)

Morphology of the fractured samples of blends and composites were studied using SEM (Hitachi S3700N VP-SEM). Post tensile fractured specimens were cut and fixed to aluminium stub, and cross-section of the sample i.e. fracture end was sputter coated with gold before imaging. Optical microscopy (Metavis U-400) was done for finding the residual fiber length in the samples post injection molding using surface polishing technique. Samples were polished carefully with fine sand paper to remove the outermost matrix layer so that fiber length can be measured accurately using optical microscope (reflection mode) and toupview software. Alternatively, matrix was burnt by keeping the composite specimens at 550 ^{o}C for 20 min. Here a sample from gripping portion of the tensile test was used. After degradation of the matrix, fibers were collected carefully, washed in acetone and dried. Since PA6, PP and *PP-g-MA* have degradation temperatures below 550 ^{o}C and carbon fibers remains stable until 2000 ^{o}C, this method was adopted to measure the residual fiber length using laser scanning confocal microscope (Leica DM18).

Grey Relational Analysis (GRA)

GRA is a statistical tool used for process optimization. In this study optimum *PP-g-MA* and SCF content required to achieve maximum tensile strength, modulus, elongation and impact strength of the composites (before water absorption) was investigated. Hence "larger-the-better" quality characteristic was used to find the Signal to Noise (S/N) ratio. Grey relational grade (GRG) was obtained from GRA using four step procedure [32]. First step is to find the S/N ratio for individual property followed by normalization of the S/N ratio data (range 0-1) and the third step is to find the grey relational coefficient for individual property (ranges between 0.5-1). Finally GRG was calculated by taking average grey relational coefficient value of tensile and impact property. In above calculations distinguishing coefficient was taken as 1.

Results and Discussion

FTIR Analysis of Blends and Composites

FTIR results of pure PA6 gave the characteristic peaks which include -NH- stretch at 3440 cm^{-1}, -CH_2- stretch at 2925 cm^{-1}, overlapping C=O stretch of amide and N-H bend of secondary amide at 1635 cm^{-1} and C-OH stretch at 1103 cm^{-1} as shown in Figure 3 [33,34]. On addition of PP, the intensity of -CH_2- stretch increased, and characteristic peaks of PP was seen at 1365 cm^{-1} and 1215 cm^{-1} representing the -CH_3- peak and -CH_2- twist respectively for the PA6/PP blend [35]. The peak intensity at 1635 cm^{-1} of PA6 shifted to 1740 cm^{-1} for PA6/PP blend which could be due to the resonance between PA6 and PP molecules [34]. Introduction of *PP-g-MA* led to absence of peak at 1740 cm^{-1} and presence of broad single peak close to 1635 cm^{-1} denoting the reaction taking place between the PA6 and *PP-g-MA* in NPM blend. The reaction between PA6 and *PP-g-MA* occurs between C-O-C of MA and -NH_2- of PA6 to form C-N-C bond as reported [36] in patent, where they have given the

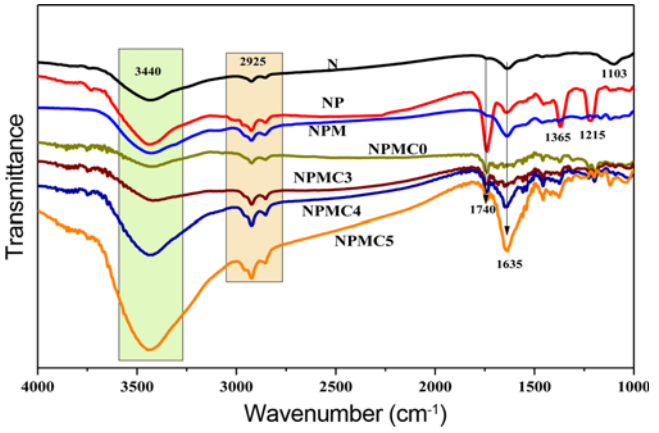

Figure 3. FTIR of N-PA6, NP-PA6/PP blend, NPM-PA6/PP/*PP-g-MA* blend, NPMC0 to NPMC5: Composites.

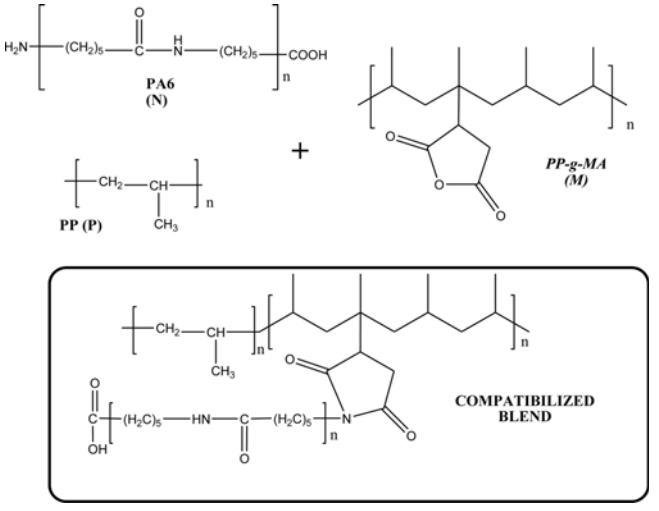

Figure 4. Reaction between PA6, PP and *PP-g-MA*, Adapted from Hergenrother *et al*. [32].

synthetic route of reaction between PA6 and *PP-g-MA*. The reaction occurring between PA6/PP blend and *PP-g-MA* has been illustrated in Figure 4.

FTIR studies of composite specimens was also carried out. When SCF was compounded along with PA6/PP blend, smaller peak at 1740 cm^{-1} and negligible peaks at 1365 cm^{-1} and 1215 cm^{-1} was observed in comparison to PA6/PP system. This reduction in peak intensity could be due to the reaction between SCF and PA6. When SCF was compounded along with PA6/PP/*PP-g-MA* blend, with increase in *PP-g-MA* content (NPMC3 to NPMC5), the intensity of -NH- peak at 3440 cm^{-1} increased as shown in Figure 3, indicating the possibility of reaction between PA6 and *PP-g-MA*, because of which there could be an increased adhesion between SCF and PA6/PP/*PP-g-MA* matrix [37]. This improvement in fiber-matrix adhesion was also observed in SEM analysis as discussed in the later section. Similar increase in peak intensity at 1635 cm^{-1} was observed with increase in *PP-g-MA* content, indicating the increased number of C=O groups from MA in the composite. Overall because of high reactivity of MA and end groups of PA6, it could be assumed that PA6 is forming bonds with both MA and SCF which could have led to compatibilization of blend and good adhesion between fiber and matrix respectively. Adhesion between fiber-matrix is important in composites, because it leads to stress transfer from matrix to the fiber indicating higher critical fiber length and better mechanical properties [38].

Tensile Properties

PA6 showed tensile strength of 49.5 MPa as shown in Figure 5. On addition of PP, the tensile strength is reduced by 26.5 % than PA6, which is due to the lower tensile strength of PP. Addition of *PP-g-MA* improved the tensile strength of PA6/PP blend by 12.2 %, but still it is 14.2 % lesser than PA6, which is also reported by Huber *et al*. [16]. The increase in the tensile strength in NPM when compared to NP could be attributed to the reduced interfacial tension between PA6 and PP [39] due to the reactivity of PA6 with *PP-g-MA* as confirmed by FTIR. Addition of SCF to PA6/PP (NPMC0) led to 10 % increase in its tensile strength in comparison to NP as shown in Figure 5. This is due to the reinforcing effect of SCF as reported in the literature [2,4,8], but the reduction in tensile strength compared to N could be due to lower compatibility of PA6/PP system. The adhesion between SCF and PA6/PP improved when compatibilizer *PP-g-MA* was used as observed from the peak intensity variation of FTIR. Addition of *PP-g-MA* led to increase in tensile strength of NPMC3 and NPMC4 (23.8 % increase compared to NPM and 30 % increase compared to NPMC0). The tensile strength was same for 3 phr & 4 phr *PP-g-MA*

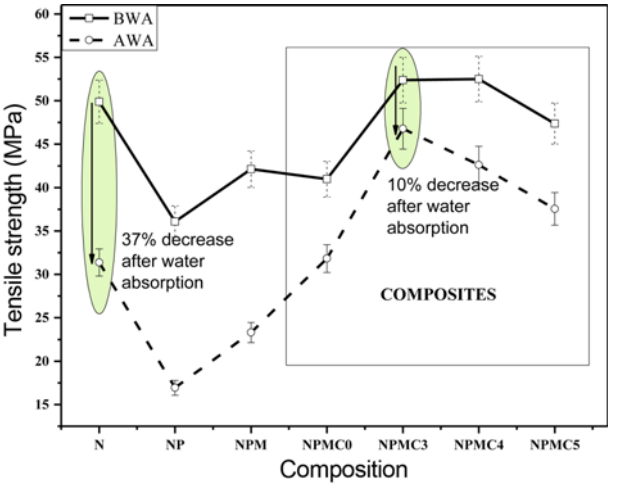

Figure 5. Variation of tensile strength of samples before (BWA) and after (AWA) water absorption. N-PA6, NP-PA6/PP blend, NPM-PA6/PP/*PP-g-MA* blend, NPMC0 to NPMC5: Composites.

compatibilized composites, but decreased for 5 phr *PP-g-MA*. The trend is similar to that of study reported by Arsad *et al*. [27], where above 2 phr compatibilizer content, the tensile strength of the blends decreased due to excess compatibilizer content.

% Elongation of pure PA6 was 300 % as illustrated in Figure 6 which confirms that PA6 is a tough engineering plastic. Inclusion of PP to PA6 drastically reduces the elongation to 12.5 % which can also be seen from the brittle fracture of PA6/PP blend. PP has low elongation and PA6/PP blend has lower resistance to crack propagation due to lower compatibility i.e. large PP globules poorly dispersed in PA6 matrix. Addition of *PP-g-MA* to PA6/PP blend increased the elongation from 12.5 to 150 % which showed the effective compatibilization of PA6/PP blend because of good dispersion of PP in PA6. Similar results were reported by other authors [40,41]. On addition of SCF to PA6/PP/ *PP-g-MA* blend, the elongation again decreased to 10 %, due to the restriction of chain mobility and brittle nature of SCF [42,43]. NPMC3 had similar % elongation as NP, but with further increase in compatibilizer content, the % elongation of composites increases slightly. Compatibilized composite NPMC5 showed 71.4 % higher elongation than NPMC0, which indicates the excessive plasticization of PA6/PP due to the presence of *PP-g-MA* [44], which also led to the reduction in tensile strength (Figure 5). The compatibilization effect is optimum in NPMC3 and NPMC4 where higher tensile strength and lower increase in elongation was observed.

Variation of stiffness for blends and composites has been illustrated in stress-strain curves shown in Figure 7. PA6 (N)

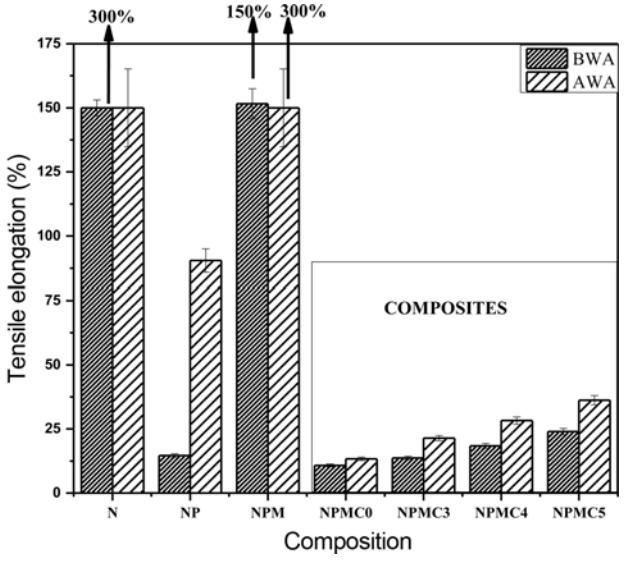

Figure 6. Variation of tensile Elongation of samples before (BWA) and after (AWA) water absorption. N-PA6, NP-PA6/PP blend, NPM-PA6/PP/*PP-g-MA* blend, NPMC0 to NPMC5: Composites.

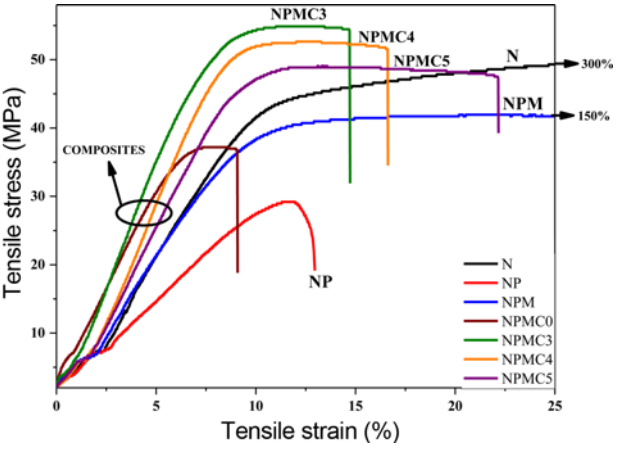

Figure 7. Representative Stress-Strain plot from tensile testing of BWA samples. N-PA6, NP-PA6/PP blend, NPM-PA6/PP/*PP-g-MA* blend, NPMC0 to NPMC5: Composites.

had less stiffness and high elongation than the composites. PA6/PP (NP) had 15 % lower modulus than N owing to lower modulus of PP. NPM had higher tensile modulus than NP as observed in tensile strength which justifies the decrement in interfacial tension due to compatibilization of PA6/PP [16]. NPMC0 had higher stiffness than N, NP and NPM due to the reinforcing effect of SCF because SCF has very high tensile modulus in comparison to matrix material. High tensile modulus was also observed for NPMC3 and it decreases slightly with increase in compatibilizer content, which proves the plasticization effect of compatibilizer as observed in SEM analysis (discussed below) and elongation measurements. From the stress-strain curve shown in Figure 7, brittle to ductile transition (increase in elongation, decrease in strength) can be observed with increase in compatibilizer content (NPMC3-NPMC4-NPMC5).

In design calculations yield strength is preferred than maximum strength for ductile materials. Considering the yield strength and yield strain values from stress-strain plots, it could be deduced that NPMC3 has 25.8 %, 35.8 % higher yield strength than N and NPM respectively. Compatibilized composites have higher yield strength values than blends and uncompatibilized (NPMC0) composites. The lowest yield strength is shown by NP, due to lack of compatibilization between PA6 and PP. Conversely, NP had highest yield strain than other blend and composites, but fractured in brittle manner without any plastic zone indicating the need of compatibilization. Compared to N and NPM, the compatibilized composites showed high yield stress, high maximum stress, low elongation and higher stiffness due to SCF and *PP-g-MA*.

Water Absorption Studies

Water absorption test showed reduction in water intake in presence of compatibilizer and SCF as shown in Table 2.

The reduction in water absorption in NP (PA6/PP) is due to the hydrophobic nature of PP, and further 16.4 % decrease in water absorption in NPM is due to the compatibilizer, as compatibilizer reacts with PA6 and reduces the free -NH_2- groups as mentioned in FTIR analysis. Water absorption of PA6 blend has been studied previously by Li *et al*. [45] and Do *et al*. [23], where the reduction in water absorption due to PBT (Polybutylene terephthalate) and PP has been reported respectively. Water absorption in PA6 is due to the free amine and the amorphous parts of PA6, where the -OH- group of water forms bond with -NH_2- group, leading to plasticization of PA6 chain. The reduced water absorption in NPMC0 might be due to the water resistant nature of SCF and PP. With addition of *PP-g-MA*, the water absorption capacity is reduced by 60 % for both NPMC3 and NPMC4 compared to N (PA6). Incorporation of 5 phr *PP-g-MA* to composite led to 64.03 % reduction in water absorption showing the combined effect of PP, SCF and the reactivity of PA6 with *PP-g-MA* and SCF.

Effect of Water Absorption (saturation) on Tensile Properties

As shown in Table 2 and Figure 5, PA6 had 37 % reduction in tensile strength and PA6/PP blend had 53 % reduction in tensile strength due to the water absorption. Same trend is followed in tensile strength values by blends and composites before and after water absorption (BWA and AWA). As expected, for NPM, the tensile strength was higher than NP, proving the effect of compatibilizer which led to lower water absorption and lesser reduction in tensile strength than NP. On addition of SCF to PA6/PP blend (NPMC0), the % reduction in tensile strength decreased from 53 % to 22 % indicating the homogeneous dispersion of SCF fibers. Surprisingly, the tensile strength values of N and NPMC0 almost became equal (32 MPa), but with the addition of compatibilizer (NPMC3) in composites the value increased to 45 MPa. For all three composites PA6/PP/*PP-g-MA*/SCF, the % reduction of tensile strength due to water saturation was between 10-20 %, least being NPMC3 composite and highest being NPMC5 composite and it might be due to plasticization of matrix by 5 phr *PP-g-MA*.

As shown in Figure 6, PA6 showed almost same % elongation after water absorption and it did not break during the test, rather slipped out of the grip due to the reduction in thickness and width during the test. An average of 2 mm reduction of thickness was observed. For PA6/PP blends, the elongation increased in comparison to BWA sample because of plasticization of PA6 phase due to water absorption, and had highest increase in elongation (>500 %) as shown in Table 2. Similar to PA6 and PA6/PP, the compatibilized blend showed 2 fold increase in elongation and this system also slipped out of the grip before break. The uncompatibilized composite which had lowest water absorption also had a lowest increase in elongation because of presence of PP and SCF, whereas the compatibilized composites had higher increase in % elongation due to plasticization of PA6 by water and *PP-g-MA* (NPMC3-56 %, NPMC4-53 %, NPMC5-50 %) but the trend of elongation change remained same BWA and AWA as shown in Figure 6.

Tensile modulus values followed the same trend as that of tensile modulus for BWA samples. The reduction in tensile modulus for AWA samples are shown in Table 2. The stiffness of all blends and composites was higher than that of PA6, showing the effect of plasticization of water on PA6 in absence of PP, *PP-g-MA* and SCF. NPM had higher modulus than N and NP. NPMC0 had lower stiffness than compatibilized composites. In both cases (blends and composites) compatibilizer is causing increase in stiffness. Compatibilized composite with 3 phr *PP-g-MA* content had highest tensile modulus than other systems similar to that of BWA samples. % reduction in stiffness due to water absorption is low for composites (30-38 %) compared to PA6 and blends (52-72 %), so these composites can be considered for applications in high humid conditions with factor of safety into consideration. From the tensile strength, elongation and stiffness values, it can be said that 3 phr *PP-g-MA* is the optimum compatibilizer content for PA6/PP/SCF system with minimum reduction in tensile strength (10 %), stiffness (30 %) and minimum increase in weight (2.4 %) due to water absorption or saturation.

Impact Strength

Comparing the impact strength values of N, NP and NPM in Figure 8, it can be seen that NPM gave highest impact strength followed by N and NP which could be due to the improved interfacial adhesion between PA6 and PP in presence of compatibilizer. The low impact strength of NP might be due to the poor dispersion of PP phase in PA6 phase as explained before. Impact strength values of the blends are matching with published results reporting that MA based compatibilizers improved the impact strength of the blends by reactive compatibilization [46,47].

Comparing composites in Figure 8, there is a slight increase in impact strength up to 4 phr compatibilizer content and then slight decrease on addition of 5 phr compatibilizer similar to that of the result observed by Huber *et al*. [16] where decrease of impact strength was seen on using higher maleated *PP-g-MA* for compatibilizing PA6/PP blend. The NPMC0 had comparable impact strength to that of NP. This indicates that SCF (5 wt % SCF) is not contributing to impact strength, but it increased the yield strength, modulus and maximum strength of the composite. NPMC4 had 1.4 % increased impact strength than NPMC3, so from Figure 8 it can be concluded that not much change in impact strength values due to the addition of compatibilizer content from 0 to 5 phr. It could also be seen that, impact strength follows the same trend as that of tensile strength in composites, which again confirms that 3 phr *PP-g-MA* content is the

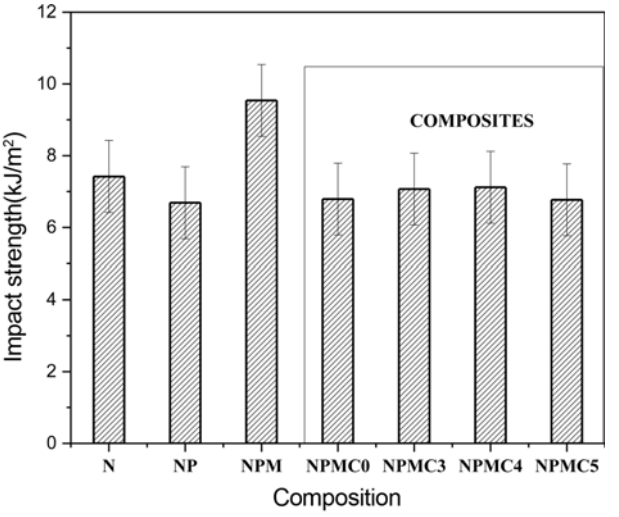

Figure 8. Variation of impact strength of sample BWA. N-PA6, NP-PA6/PP blend, NPM-PA6/PP/*PP-g-MA* blend, NPMC0 to NPMC5: Composites.

optimized compatibilizer content for PA6/PP/SCF composite.

SEM Fractography and Measuring Residual Fiber Length Using OM and CLSM

From SEM fractography shown in Figure 9, it can be said that PA6 under tensile load failed due to excessive pull out (Figure 9(a)). PA6/PP (NP) had a smooth fracture across the width showing no pull out of matrix, which could be due to the brittle nature of PP as observed from elongation measurements (only 12 % elongation for PA6/PP compared to 300 % elongation for PA6). It can be said that crack initiated and propagated at the PP interface because it is not bonded well to PA6. When compatibilizer was added to PA6/PP blend; it showed again pull-out on the fractured surface as it is noticed in the case of PA6 (elongation also increased to 150 %; Figure 9(c)), but the intensity of pull out is low in comparison to PA6 indicating the reaction between PA6- *PP-g-MA*- PP. Because of the brittle nature of SCF and bonding between SCF and PA6, little matrix pull out could be seen in NPMC0 system, which showed brittle fracture like NP with exception of slightly fibrillated PA6 because of phase difference existing between PA6 and PP (Figure 9(d)).

SEM images of fractured composite specimens are shown in Figure 10. Comparing the fractography of compatibilized composite systems, the SCF gets more wetted and adhered into the matrix system as seen in Figure 10(d), where the fiber is fully surrounded by the matrix. The interfacial adhesion between the fiber (SCF) and matrix (PA6/PP/*PP-g-MA*) is clearly seen in Figure 10(d) because cohesive failure of the matrix is observed. For 3 phr and 4 phr compatibilizer content, little matrix pull out and transverse fracture of matrix could be the reason for composite failure, but in the case of 5 phr compatibilizer, matrix shearing led to composite fracture. Comparing NPMC0-NPMC5 (Figure 9(d), 10(a) to 10(d)) fractographs, thread like appearance has turned to network or web like appearance, which could be due to the increased interfacial adhesion between the PA6/PP and compatibilizer. It is also seen that higher amount of compatibilizer leads to poor dispersion of SCF due to the web like appearance of the matrix, and it also resulted in reduction of tensile strength and increase in elongation of the composite system. SCF are circled in Figure 10(d) indicating the fiber diameter of 7 μm. For 5 phr *PP-g-MA* content, the

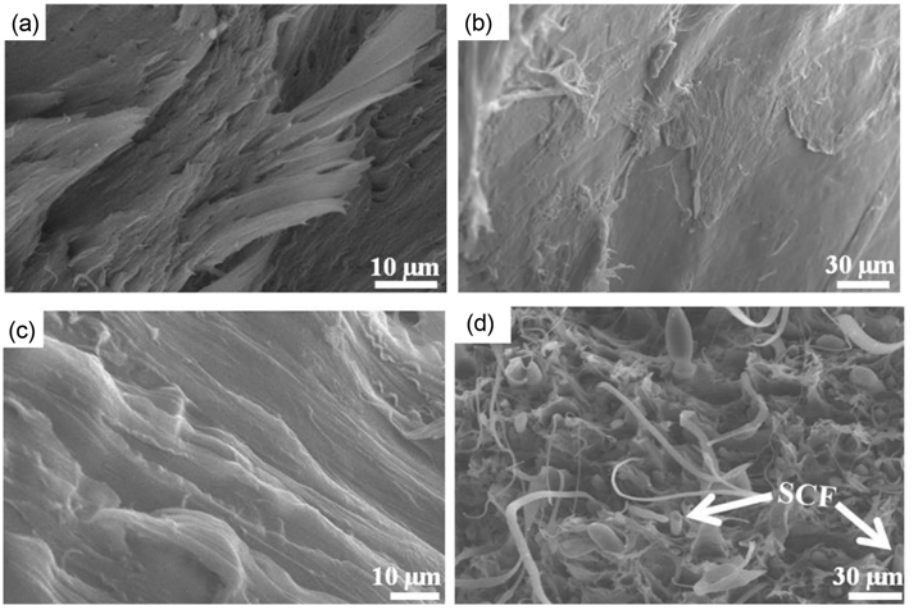

Figure 9. SEM images of tensile fractured surface of (a) N-PA6, (b) NP-PA6/PP, (c) NPM-PA6/PP/*PP-g-MA*, and (d) NPMC0-PA6/PP/SCF.

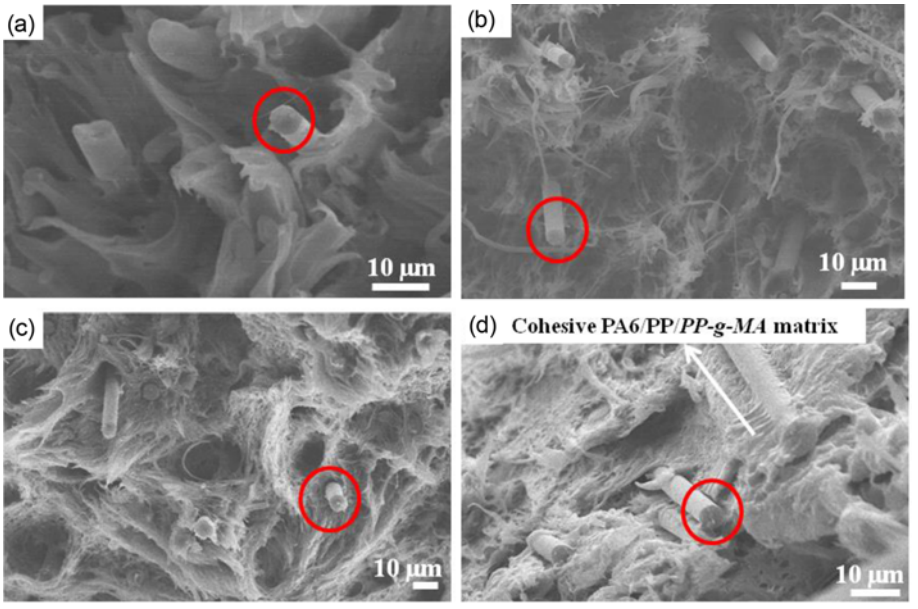

Figure 10. SEM images of tensile fractured surface of (a) NPMC0-PA6/PP/SCF (b) NPMC3-PA6/PP/*PP-g-MA* (3 phr)/SCF, (c) NPMC4-PA6/PP/*PP-g-MA*(4 phr)/SCF, and (d) NPMC5-PA6/PP/*PP-g-MA*(5 phr)/SCF. Circles denote the carbon fibers.

composite had ductile failure, showing the plasticizing effect of *PP-g-MA* on PA6/PP/SCF. SEM results correlates well with the FTIR and tensile results, showing that the increase in compatibilizer content is causing gradual change in fracture pattern from brittle to ductile nature in composites.

Composite strength and stiffness depends on fiber diameter, residual fiber length especially when extrusion and injection molding are involved due to their extreme shearing effects. Residual fiber length should be equal or higher than the critical fiber length to get the reinforcing effect of fibers. Since no change in fiber diameter was observed (Figure 10(d)), only fiber lengths and their distribution in all composites were studied. From the surface polishing method (not shown) it could be understood that the average residual fiber length varies from 50-125 μm, lowest being for NPMC3, followed by NPMC4 and then by NPMC5 composites. Average fiber length of more than 100 μm was observed for NPMC0 which does not have any compatibilizer, which could be due to lower interaction between PA6 and PP. Zhang *et al*. [22] reported a critical fiber length of 260 μm for PA6/SCF composite, but no data has been reported as per our knowledge for PA6/PP/*PP-g-MA*/SCF composite.

Figure 11(a) shows the residual fibers in a composite

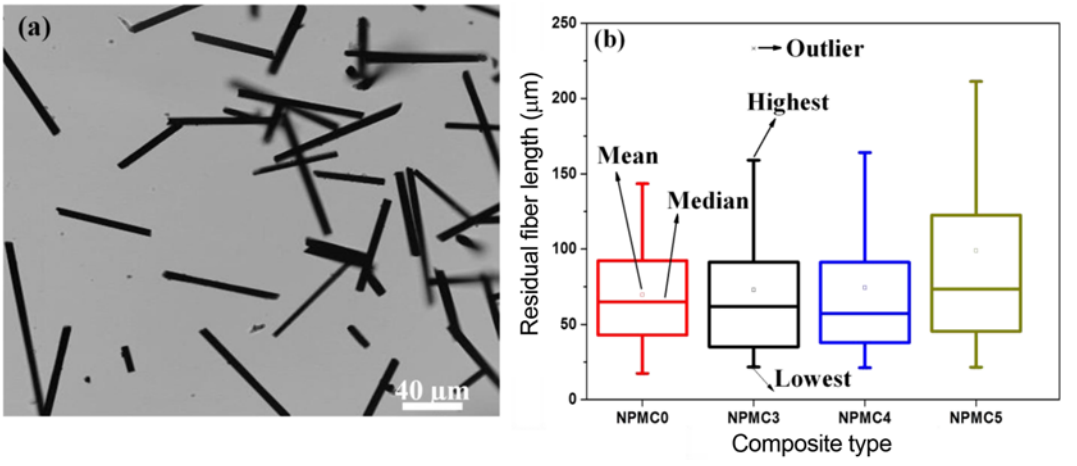

Figure 11. Residual fiber length of Short carbon fibers (SCF) after burning the matrix; (a) confocal laser scanning microscopic image of individual SCF fibers after burning the matrix in NPMC3 composite (b) box and whiskers plot showing residual fiber length of all composites measured using image J software after capturing the image as shown in (a).

Table 3. (a) Factors and their assigned Levels considered Grey Relational Analysis (GRA)

Control factors	Level 1	Level 2	Level 3	Level 4
PP-g-MA (phr)	0	3	4	5
SCF (wt %)	0	5		

Table 3. (b) Response table for Grey Relational Grade. Bold figures represent the higher (optimal) value. Total mean value of the GRG is 0.7186. Note that SCF is more influencing than PP-g-MA on tensile and impact properties

Control factors	Level 1	Level 2	Level 3	Level 4	Difference (Max-Min)	Rank
PP-g-MA (phr)	0.6751	**0.7477**	0.7389	0.7130	0.0726	2
SCF (wt %)	0.6587	**0.7787**			0.1200	1

(NPMC3) after removing the matrix. Similarly, the residual fiber lengths (50 readings) of each composite were measured and represented as a box and whiskers plot in Figure 11(b). This plot gives the lowest, highest and mean value of the residual fiber lengths of the each composite. It could be understood that the average residual fiber length is same as that of surface polishing method, but the highest values were observed for NPMC5 composite. Slight increase in residual fiber length was observed with increase in compatibilizer content and average residual fiber length was found to be around 75 μm. The reduction in average fiber length (almost from 1000 μm to 75 μm) is due to breakage occurring in extrusion and injection molding as the fiber is very weak in transverse direction and shearing effects involved in compatibilization. It is assumed that ~75 μm of residual fiber length is almost equal to the critical fiber length of SCF fibers in PA6/PP/*PP-g-MA*/SCF composite because 140 % increase in tensile strength (after water saturation) was observed with the addition of SCF fibers. Zhang *et al*. [22] also reported the reduction of the fiber length from 12 mm to 1.9 mm for PA6/ 5 wt % CF composite processed via melt pultrusion followed by injection molding and their study showed that fiber length is decreasing further with increase in wt % of CF. Hence to obtain the reinforcing effect of the fibers, it is important to increase the residual fiber length of the SCF fibers to above their critical fiber lengths by adjusting the processing parameters, which is a challenging especially during extrusion.

Statistical Analysis Using GRA Method

PP-g-MA content (0, 3, 4 and 5 phr) and SCF (0 and 5 %) content were chosen as factor-level combinations as shown in Table 3(a), which are the input parameters considered in the GRA analysis. Tensile strength, tensile modulus, elongation and impact strength are considered as output responses. With two factors and four levels, the number of experiments is eight, and the corresponding GRG for all output responses were found as explained in experimental section. The factor and level having highest GRG is considered as the optimum parameter for obtaining better combination of mechanical properties.

From the GRG value as tabulated in Table 3(b), higher value of GRG is observed for 3 phr *PP-g-MA* content and 5 wt% SCF content. As the GRG values are well above 0.5, it could be said that both *PP-g-MA* content and SCF content plays a major role in determining the mechanical properties of the composites. To affirm this, the difference between maximum and minimum value among levels was found, and the rank was given. From the difference it can be seen that the *PP-g-MA* has Rank 2 and SCF has Rank 1 denoting that SCF content plays better role than *PP-g-MA* content in determining the mechanical properties of PA6/PP/*PP-g-MA*/ SCF composites. Overall from GRA analysis, it is understood that for obtaining higher strength, stiffness and toughness, 3 phr *PP-g-MA* and 5 wt% SCF is the most optimum composition which corroborates with the experimental data where NPMC3 was considered to be the most optimum composition as shown in Figure 5, 7, 8 and 10. Despite the fiber breakage during processing, the contribution of SCF is slightly better than the *PP-g-MA* content in obtaining optimum composite properties as seen from Table 3b, but for obtaining stiffer composite higher SCF content and for obtaining tougher composite higher *PP-g-MA* content should be used.

Conclusion

Effect of *PP-g-MA* compatibilizer content on properties of PA6/PP/SCF composites with and without water saturation has been studied with the aim of using tough composites in under water applications such as pressure vessels or high humid environments such as automobile exterior components. FTIR studies proved the occurrence of reaction between PA6 and *PP-g-MA*. For PA6/PP/*PP-g-MA*/SCF composites, with increase in the compatibilizer content from 3 phr to 5 phr, strength, stiffness and impact strength decreased slightly, but the elongation increased. Around 40 % increase in tensile strength was observed due to the effect of 5 wt % SCF reinforcement. From SEM fractographs it was found that brittle fracture was seen for PA6/PP/SCF system, but with the addition of compatibilizer, the fracture patterns were more of ductile in nature (matrix pull out) indicating the

good interfacial adhesion within the matrix (blend) and also between matrix and fiber. But at higher *PP-g-MA* content (5 phr), the matrix gets plasticized leading to early yielding and low tensile strength of the composite system. Fiber breakage during processing resulted in residual fiber length of around 75 μm in case of composites with 3 phr or 4 phr compatibilizer and 100 μm in the case of 5 phr compatibilizer. From the experimental results, it was found that 3 phr *PP-g-MA* is the optimum compatibilizer content for PA6/PP/SCF composites which was also confirmed using Grey relational analysis.

Tensile properties after water saturation were also studied in detail. With the addition of compatibilizer, PA6/PP/*PP-g-MA*/SCF composite showed around 50 % increase in tensile strength in comparison to pure PA6 after water saturation. The composite containing 3 phr *PP-g-MA* had only 10 % reduction in tensile strength, 30 % reduction in modulus and 56 % increase in elongation due to water absorption in comparison to dry sample of same composition. Hence, usage of PA6/PP/*PP-g-MA*/SCF composite can be expanded to components used in underwater or high humid applications with factor of safety taken into consideration. It can be concluded that 3-phr *PP-g-MA* is suitable for obtaining optimum composite properties and further improvement in properties could be achieved by studying various other parameters such as fiber content, residual fiber length and processing techniques.

References

1. H. Luo, G. Xiong, C. Ma, D. Li, and Y. Wan, *Mater. Des.*, **64**, 294 (2014).
2. N. G. Karsli and A. Aytac, *Compos. Part B: Eng.*, **51**, 270 (2013).
3. E. C. Botelho, L. Figiela, M. C. Rezende, and B. Lauke, *Compos. Sci. Tech.*, **63**, 1843 (2003).
4. S. Zhou, Q. Zhang, C. Wu, and J. Huang, *Mater. Des.*, **44**, 493 (2013).
5. C. E. Pelin, A. Stefan, I. Dincă, A. Ficai, G. Pelin, E. Andronescu, D. Constantinescu, and G. Voicu, *J. Optoelectron. Adv. M.*, **17**, 750 (2015).
6. H. Li, Y. Wang, C. Zhang, and B. Zhang, *Compos. Part A: Appl. Sci. Manuf.*, **85**, 31 (2016).
7. H. J. An, J. S. Kim, K. Ki-Young, D. Y. Lim, and D. H. Kim, *Fiber. Polym.*, **15**, 2355 (2014).
8. S. Molnár, J. Gulyás, and P. Béla, *J. Macromol. Sci. B*, **38**, 721 (1999).
9. C. Brauner, A. S. Herrmann, P. M. Niemeier, and K. Schubert, *J. Thermoplast. Compos. Mater.*, **30**, 302 (2017).
10. A. Gonzalez-Montiel, H. Keskkula, and D. R. Paul, *Polymer,* **36**, 4605 (1995).
11. A. Gonzalez-Montiel, H. Keskkula, and D. R. Paul, *J. Polym. Sci. B: Polym. Phys.*, **33**, 1751 (1995).
12. B. Ohlsson, H. Hassander, and B. Tornell, *Polymer*, **39**, 6705 (1998).
13. F. P. L. Mantia and C. Mongiovi, *Polym. Degrad. Stab.*, **66**, 337 (1999).
14. F. Ide and A. Hasegawa, *J. Appl. Polym. Sci.*, **18**, 963 (1974).
15. D. Fu, T. Kuang, F. Chen, L. J. Lee, and X. Peng, *Mater. Chem. Phys.*, **164**, 1 (2015).
16. T. Huber, M. Misra, and A. K. Mohanty, *J. Appl. Polym. Sci.*, **131**, 40792 (2014).
17. S. George, K. Ramamurthy, J. S. Anand, G. Groeninckx, K. T. Varughese, and S. Thomas, *Polymer*, **40**, 4325 (1999).
18. L.-F. Ma, X.-F. Wei, Q. Zhang, W.-K. Wang, L. Gu, W. Yang, B.-H. Xie, and M.-B. Yang, *Mater. Des.*, **33**, 104 (2012).
19. S. Thomas and G. Groeninckx, *Polymer*, **40**, 5799 (1999).
20. J. Abraham, K. Muraleedharan, C. Radhesh Kumar, S. Thomas, and S. C. George, *Polym. Eng. Sci*., **57**, 231 (2017).
21. F. Rezaei, R. Yunus, N. A. Ibrahim, and E. D. Mahdi, *Polym.-Plast. Tech. Eng.*, **47**, 351 (2008).
22. S. Zhang, X. Wang, and D. Wu, *Polym. Compos.*, **37**, 2705 (2016).
23. V.-T. Do, H.-D. Nguyen-Tran, and D.-N. Chun, *Compos. Struct.*, **150**, 240 (2016).
24. S.-J. Park and M.-K. Seo in "Polymer Composites, Volume 1: Macro and Micro Composites" (S. Thomas, K. Joseph, S. K. Malhotra, K. Goda, and M. S. Sreekala Eds.), pp.137-180, Wiley-VCH Verlag & Co, Germany, 2012.
25. W. S. Chow, Z. M. Ishak, J. Karger-Kocsis, A. A. Apostolov, and U. S. Ishiaku, *Polymer*, **44**, 7427 (2003).
26. H. J. Zo, S. H. Joo, T. Kim, P. S. Seo, J. H. Kim, and J. S. Park, *Fiber. Polym.*, **15**, 1071 (2014).
27. A. Arsad, A. R. Rahmat, A. Hassan, and S. N. Iskandar, *J. Reinf. Plast. Compos.*, **29**, 2808 (2010).
28. I. Gonzalez, J. I. Eguiazabal, and J. Nazabal, *Eur. Polym. J.*, **42**, 2905 (2006).
29. H. Balakrishnan, A. Hassan, N. A. Isitman, and C. Kaynak, *Polym. Degrad. Stab*., **97**, 1447 (2012).
30. P. Davies, P.-Y. L. Gac, M. L. Gall, and M. Arhant in "Durability of Composites in a Marine Environment 2" (P. Davies and Y. D. S. Rajapakse Eds.), pp.225-234, Springer, Switzerland, 2018.
31. A. Oromiehie, H. Ebadi-Dehaghani, and S. Mirbagheri, *Int. J. Chem. Eng. Appl.*, **5**, 117 (2014).
32. K. Krishnaiah and P. Shahabudeen, "Applied Design of Experiments and Taguchi Methods", pp.273-296, PHI Learning Private Limited, India, 2012.
33. M. Nasir, I. Mohammad, H. Asad, and S. Shaukat, *Polymer*, **5**, 1380 (2013).
34. K. Amir and P. Mazeyar, *J. Appl. Polym. Sci.*, **116**, 3140 (2010).
35. J. H. Lin, Y. J. Pan, C. F. Liu, C. L. Huang, C. T. Hsieh, C. K. Chen, Z. I. Lin, and C. W. Lou, *Materials*, **8**, 8850 (2015).

36. W. L. Hergenrother, M. G. Matlock, and R. J. Ambrose, *U.S. Patent*, 4427828 (1986).
37. N. Feng, X. Wang, and D. Wu, *Curr. Appl. Phys.*, **13**, 2038 (2013).
38. R. B. Adusumalli, M. Reifferscheid, H. K. Weber, T. Roeder, H. Sixta, and W. Gindl, *J. Compos. Mater.*, **46**, 359 (2012).
39. A. Gonzalez-Montiel, H. Keskkula, and D. R. Paul, *Polymer*, **36**, 4587 (1995).
40. P. Agrawal, A. W. Rodrigues, E. M. Araújo, and T. J. Mélo, *J. Mater. Sci.*, **45**, 496 (2010).
41. R. A. Kudva, H. Keskkula, and D. R. Paul, *Polymer*, **40**, 6003 (1999).
42. S. C. Tjong and Y. Z. Meng, *Polymer*, **40**, 1109 (1999).
43. B. Li, Y. Zhang, X. Bai, S. Wang, and J. Ji, *J. Polym. Sci. B: Polym. Phys.*, **47**, 2188 (2009).
44. S. K. Sharma and S. K. Nayak, *Polym. Degrad. Stab.*, **94**, 132 (2009).
45. H. Li, J. Wang, G. Li, Y. Lu, N. Wang, Q. Zhang, and X. Qu, *Polymer Adv. Tech.*, **28**, 699 (2017).
46. D. Purnima, S. N. Maiti, and A. K. Gupta, *J. Appl. Polym. Sci.*, **102**, 5528 (2006).
47. S. Aparna, D. Purnima, and R. B. Adusumalli, *Polym.-Plast. Tech. Eng.*, **56**, 617 (2017).